Methods for Expansion of 3-Loop 2-Point Feynman Integrals

E. de Doncker[1(✉)], F. Yuasa[2], T. Ishikawa[2], and K. Kato[3]

[1] Western Michigan University, Kalamazoo, MI 49008, U.S.A.
elise.dedoncker@wmich.edu
[2] High Energy Accelerator Research Organization (KEK), Ibaraki 1-1 OHO Tsukuba, 305-0801, Japan
{fukuko.yuasa,tadashi.ishikawa}@kek.jp
[3] Department of Physics, Kogakuin University, Shinjuku, Tokyo 163-8677, Japan
katok@kute.tokyo

Abstract. We explore various approaches to expand 3-loop 2-point Feynman integrals with respect to the dimensional regularization parameter. These methods are tailored to the range of the squared momentum. Below a threshold in the squared momentum, we can use lattice integration rules and a linear extrapolation for the integral expansion. An expansion of the integrand and adaptive integration of the individual terms can also be employed. We further rely on the latter techniques for the computations above the threshold.

Keywords: Feynman loop diagrams · dimensional regularization · adaptive/non-adaptive integration · lattice rules · GPUs

1 Introduction

Marked improvements in the technology of high energy physics experiments impose the need for accurate theoretical predictions, which can be contributed by higher-order corrections in the perturbation method.

The Feynman diagrammatic approach introduces Feynman loop integrals in the calculation of higher-order corrections to the cross section of particle interactions. The one-loop level has been completely established in an analytic manner [13] and implemented in packages such as LoopTools [12]. A general and analytic treatment is not possible for multi-loop integrals with general mass and momentum values.

Although challenging Feynman integral computations can presently be performed using existing symbolic or symbolic/numerical software packages such as pySecDec [2], we target the development of fully numerical methods using "automatic" integration strategies that require little or no knowledge of the problem or the underlying numerical analysis.

The scalar loop integral is defined as

$$\mathbf{I} = \prod_{k=1}^{L} \int \frac{d^{\nu}\ell_k}{(2\pi)^{\nu}} \frac{1}{D_1 \cdots D_N} \tag{1}$$

© The Author(s), under exclusive license to Springer Nature Switzerland AG 2026
O. Gervasi et al. (Eds.): ICCSA 2025 Workshops, LNCS 15890, pp. 20–30, 2026.
https://doi.org/10.1007/978-3-031-97606-3_2

where $D_r = p_r^2 - m_r^2$ is the inverse propagator of the r-th internal line with mass m_r, N is the number of lines, and L is the number of loops. When we deal with the UV singularity by dimensional regularization, the space-time dimension, ν, is set to $4 - 2\varepsilon$.

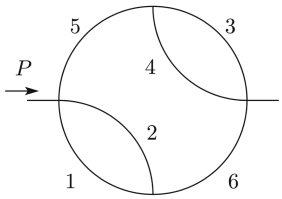

Fig. 1. 3-loop *baseball* diagram with $N = 6$ lines. The numbers denote the index r in Eq. (2).

Subsequently we explore 3-loop 2-point integrals associated with the "baseball" diagram of Fig. 1 with $N = 6$ internal lines and the external momentum P. According to the Nakanishi formalism [3,16], for $L = 3$ and $N = 6$ and without the prefactor, we denote

$$\mathcal{I} = \int_{\mathcal{C}_6} \prod_{r=1}^{6} dx_r \, \delta(1 - \sum x_r) \, U^{\,\varepsilon - 2} (V - i\varrho)^{-3\varepsilon} \tag{2}$$

where x_r is the Feynman parameter of the r-th internal line, $V = M^2 - sW/U$ with squared momentum $s = P^2$, $M^2 = \sum_r m_r^2 x_r$; U is an L-th order polynomial of x_r and W is of order $(L+1)$; ε is an infinitesimal parameter, and (with the goal to obtain an approximation), it is the objective to expand $\mathcal{I}$ as a series in powers of ε. We include ϱ also as an infinitesimal parameter, which is set to 0 unless V vanishes in the domain; in the latter case, an extrapolation with respect to ϱ can help alleviate the effect of some singularities within the domain. $\mathcal{C}_d$ is the d-dimensional unit hypercube. In the dimensional regularization method the integral is given by the Laurent series in ε of the form

$$\mathcal{I} = \frac{C_{-2}}{\varepsilon^2} + \frac{C_{-1}}{\varepsilon} + C_0 + C_1\varepsilon + \cdots . \tag{3}$$

Here, C_{-2}, C_{-1}, C_0 and C_1 are leading expansion coefficients. In this paper we focus on the numerical expansion with respect to ε and the behavior of the coefficients as a function of s and we compute the equal mass case as $m_r = m, 1 \le r \le 6$.

In integral computations, transformations are basic tools to simplify the integrand and/or smoothen its behavior (see also Sect. 3.4). We perform the variable transformation $x_r = y_r$, $1 \le r \le 4$ and $x_5 = y_5 z$, $x_6 = y_5 \bar{z}$ where $\bar{z} = 1 - z$. The U and W can be written as follows:

$$U = y_1y_2y_3 + y_1y_2y_4 + y_1y_3y_4 + y_2y_3y_4 + (y_1 + y_2)(y_3 + y_4)y_5 \tag{4}$$

$$W = y_1y_2y_3y_4 + y_1y_2(y_3 + y_4)y_5z + (y_1 + y_2)y_3y_4y_5\bar{z} + (y_1 + y_2)(y_3 + y_4)y_5^2 z\bar{z}. \tag{5}$$

In our previous work [6,7], several 3-loop diagrams and their associated integrals were treated analytically and numerically after separating the ultra-violet divergence by use of the sector decomposition(SD) method.

For the diagram in Fig. 1, we divide the integration region R

$$R = \{(y_1, y_2, y_3, y_4, y_5) \mid \sum_{j=1}^{5} y_j = 1\} \tag{6}$$

into regions $R(k, l, m, n, p)$.

In this decomposition, the integrals are labeled by the $120 = 5!$ permutations of the quintuple $(1, 2, 3, 4, 5)$, but only fifteen distinct cases (regions) remain after taking symmetries into account. We studied the $\mathcal{I}_{51234}$ integral in [7]. In this paper, we will demonstrate our numerical techniques for $\mathcal{I}_{12345}$ and $\mathcal{I}_{12534}$. We have already touched on a preliminary study for the full calculation of the 15 regions and it shall be presented in a future publication.

In the region $R(k, l, m, n, p)$, the variables are transformed as

$$y_k = s_k, \quad y_l = s_k t_l, \quad y_m = s_k t_l u_m, \quad y_m = s_k t_l u_m v_n, \quad y_p = s_k t_l u_m v_n w_p \tag{7}$$

where $0 \le t_l, u_m, v_n, w_p \le 1$ and $s_k^{-1} = 1 + t_l(1 + u_m(1 + v_n(1 + w_p)))$. Hereafter, we omit the index for t, u, v, w when it is redundant.

The U function is a sum of monomials and each monomial is a product of three different y's with coefficient 1. We call a region $R(k, l, m, n, p)$ and the corresponding integral in the region as Type-I(II) when the term $y_k y_l y_m$ is (not) in U[1]

The U and W functions are

$$\begin{array}{l} U = s_k^3 t^2 uf, \;\; W = s_k^4 t^2 uq, \;\; (\text{Type} - \text{I}) \\ U = s_k^3 t^2 uvf, \, W = s_k^4 t^2 uvq, \, (\text{Type} - \text{II}) \, , \end{array} \tag{8}$$

$$V s_k^{-1} = G = m^2\, g - s\frac{q}{f}, \qquad h = y_5 s_k^{-1}, \qquad g = (1+t(1+u(1+v(1+w)))) \tag{9}$$

where functions f, q, G, h are defined.

Section 2 will specify the integrals in detail. Section 3 will develop the methods used, based on lattice-rule non-adaptive integration, and an iterated adaptive method. Results will be presented in Sect. 4 and Conclusions in Sect. 5.

2 Integrals

Summed over the regions, the integral of Eq. (2) becomes $\mathcal{I} = \sum_\alpha \mathcal{I}_\alpha$, with $\alpha = (k, l, m, n, p)$; here we focus on $\mathcal{I}_{12345}$ of Type-I and $\mathcal{I}_{12534}$ of Type-II. The variable transformation in SD works to specify the ultra-violet divergence clearly. As shown in the following equations, in Type-I, the t-integral is of order $1/\varepsilon$, while in Type-II both the t- and v- integrals are in $1/\varepsilon$. The singularity can be softened by a factor h. Then for $\mathcal{I}_{12345}$ of Type-I the Laurent series in Eq.(3) starts from the C_0 term and for $\mathcal{I}_{12534}$ of Type-II the series starts from C_{-1}. With $H = G^{-3\varepsilon}/f^{2-\varepsilon}$, these are given by

$$\begin{aligned} &\mathcal{I}_{12345} = \int_{\mathcal{C}_5} dz\, dt\, du\, dv\, dw\; h\, v\, t^{2\varepsilon-1} u^\varepsilon H, \quad \text{with} \\ &h = tuvw, \\ &f = 1 + v + uv(1 + w + vw + t + tw + tvw), \\ &q = tuv(1 + wz + vwz + uvw\bar{z} + uvw^2\bar{z}z + uv^2w^2\bar{z}z + \\ &tuvw\bar{z} + tuvw^2\bar{z}z + tuv^2w^2\bar{z}z), \end{aligned} \tag{10}$$

[1] In Ref [6], we studied the case of a 'complete' U function, which is the sum of all possible monomials. In this case, all regions are Type-I and the f in Eq. (8) is identical for all regions.

and

$$\mathcal{I}_{12534} = \int_{\mathcal{C}_5} dz\, dt\, du\, dv\, dw\; h\, v^{\varepsilon-1}\, t^{2\varepsilon-1} u^{\varepsilon} H, \quad \text{with} \tag{11}$$
$$h = tu,$$
$$f = 1 + w + u + uw + uvw + tu + tuw + tuvw,$$
$$q = tu(z + wz + vw + u\bar{z}z + uw\bar{z}z + uvw\bar{z} + tu\bar{z}z + tuw\bar{z}z + tuvw\bar{z}).$$

$\mathcal{I}_{12534}$ can further be expressed as

$$I = I_0 + I_1 \quad \text{with} \tag{12}$$
$$I_0 = \int_0^1 dz \int_0^1 dt \int_0^1 du \int_0^1 dw \frac{1}{\varepsilon} \frac{(h/t)}{t^{-2\varepsilon} u^{-\varepsilon}} \frac{G_b^{-3\varepsilon}}{f_b^{2-\varepsilon}}, \tag{13}$$
$$I_1 = \int_0^1 dz \int_0^1 dt \int_0^1 du \int_0^1 dv \int_0^1 dw \frac{(h/t)}{t^{-2\varepsilon} u^{-\varepsilon} v^{1-\varepsilon}} \left(\frac{G^{-3\varepsilon}}{f^{2-\varepsilon}} - \frac{G_b^{-3\varepsilon}}{f_b^{2-\varepsilon}} \right), \tag{14}$$

where the h, f, f_b ($f_b = f|_{v=0}$), G and G_b ($G_b = G|_{v=0}$) functions are different for each case.

Note that, for $\mathcal{I}_{12345}$, we will expand the integral with respect to ε using a linear extrapolation (see Sect. 3.3), whereas for $\mathcal{I}_{12534}$ we expand the integrands of I_0 and I_1. The integrands F_0 of I_0 and F_1 of I_1 can be expanded with respect to ε as

$$\begin{aligned} F_0 \sim\ & \frac{h}{f_b^2 t} \frac{1}{\varepsilon} + \frac{h}{f_b^2 t} (\log f_b - 3 \log G_b + 2 \log t + \log u) \\ & + \frac{h}{2 f_b^2 t} [\ \log^2 f_b - 6 \log f_b \log G_b + 9 \log^2 G_b + 4 \log f_b \log t \\ & - 12 \log G_b \log t + 4 \log^2 t + 2 \log f_b \log u - 6 \log G_b \log u \\ & + 4 \log t \log u + \log^2 u\ ]\, \varepsilon \\ & + \mathcal{O}(\varepsilon^2) \end{aligned} \tag{15}$$

and

$$\begin{aligned} F_1 \sim\ & \frac{h}{tv} \left(\frac{1}{f^2} - \frac{1}{f_b^2} \right) - \frac{h}{f^2 f_b^2 tv} [-{f_b}^2 \log f + f^2 \log f_b + 3{f_b}^2 \log G - 3 f^2 \log G_b \\ & + 2 f^2 \log t - 2 f_b^2 \log t + f^2 \log u - f_b^2 \log u + f^2 \log v - f_b^2 \log v] \varepsilon \\ & + O(\varepsilon^2). \end{aligned} \tag{16}$$

With these expansions, we can integrate each term analytically and/or numerically. The first term of (15) corresponding to C_{-1} of I_0 is s-independent and it can be integrated numerically by Mathematica or other numerical integration methods. The second and the third term of (15) corresponding to C_0 and C_1 of I_0 include s-independent and s-dependent parts and as a whole they are s-dependent. Similarly, C_0 of I_1 in (16) is s-independent and C_1 of I_1 is s-dependent. Table 1 indicates the s-dependency of each coefficient.

Table 1. s-dependency of expansion coefficients

	C_{-1} real	C_0 real	C_1 real	C_{-1} imag.	C_0 imag.	C_1 imag.
I_0	s-independent (constant value)	s-dependent	s-dependent	-	s-dependent	s-dependent
I_1	-	s-independent (constant value)	s-dependent	-	-	s-dependent

3 Numerical Methods

3.1 Rank-1 Lattice Rules

Eliminating the δ-function in (2) yields an integral over an $(N-1)$-dimensional simplex, which can then be transformed to the $(N-1)$-dimensional unit cube. Lattice rules are applied with a periodizing transformation that flattens the integrand at the boundaries of the cube. A rank-1 lattice rule is given by $Qf = \frac{1}{n}\sum_{j=0}^{n-1} f(\{\frac{j}{n}\mathbf{z}\})$ where n is the number of integrand evaluations (see, e.g., [22]). Here $\mathbf{z}$ is an integer *generator* vector of length d with components $z \in \mathcal{Z}_n = \{1 \le z < n \mid gcd(z,n) = 1\}$, where $\{\mathbf{x}\}$ denotes the vector obtained by taking the fractional part of each component of $\mathbf{x}$. Classically n is prime [14,15] and $\mathcal{Z}_n = \{1, 2, \ldots, n-1\}$. We precomputed the generators $\mathbf{z}$ for various numbers of points n using the component by component (CBC) algorithm [17,18]. The CBC algorithm runs in $\mathcal{O}(d\,n\,\log(n))$ time and $\mathcal{O}(n)$ space.

3.2 Composite/embedded Lattice Rules

An embedded sequence is given in [22], based on m copies of a rank-1 rule in r coordinate directions; m and n are assumed relatively prime.

Q_r is the m^r-copy rule of the original rule; has $m^r n$ points and is of rank r for $1 \le r \le d$. The points of Q_r are embedded in those of Q_{r+1}. An error estimate is also calculated.

Because of their regular structure, lattice rules are very well-suited for parallelization on GPUs (see, e.g., [1,4] implemented on Kepler-20 GPU. For the GPU computations we used CUDA, where the rule evalutions are laid out over the GPU cores. Later work included [8,11]. For this paper we made use of a GV100 Quadro GPU, which is specified with 5120 CUDA cores, 80 SMs, 32 GB of memory, and bandwidth of 868.4 GB/s. The theoretical performance is fast at 8.33 TFLOPS for FP64 (double). It is 33.32 TFLOPS for FP16 (half), and 16.66 TFLOPS for FP32 (float).

Note that an adaptive procedure is much harder to implement on a many-core system (see, e.g., [9]).

3.3 Linear Extrapolation

Linear extrapolation for an integral $\mathcal{I}$ is based on an asymptotic expansion of the form

$$\mathcal{I}(\varepsilon) \sim \sum_{k \ge \kappa} C_k\, \varphi_k(\varepsilon), \qquad \text{as } \varepsilon \to 0$$

where the sequence of $\varphi_k(\varepsilon)$ is known. The expansion is truncated after $2, 3, \ldots$ terms to form linear systems of increasing size in the C_k variables.

3.4 Transformations

For an integral $\mathcal{I}f = \int_0^1 f(x)\,dx$, we use a periodizing transformation $x = \Psi_p(t)$ of rather high order, $p = 6$ [20,21], so that the function can be extended periodically and which will help alleviate boundary singularities. We have

$$\Psi_p(t) = \frac{\theta_p(t)}{\theta_p(1)}, \quad \text{where}$$
$$\theta_p(t) = \int_0^t \sin^p(\pi u)\,du, \quad p = 1, 2, \ldots,$$

in particular,

$$\Psi_6(t) = t - (45\sin(2\pi t) - 9\sin(4\pi t) + \sin(6\pi t))/(60\pi)$$
$$\text{with } \Psi_6'(t) = \frac{16}{5}\sin^6(\pi t). \tag{17}$$

3.5 Iterated Automatic Adaptive Integration

The goal of automatic integration is to employ a blackbox approach to approximate integrals. For a user-specified function, required accuracy and a limit on the number of integrand evaluations, the procedure seeks to return an approximation $\mathcal{Q}f$ to an integral $\mathcal{I}f$, and estimated error $\mathcal{E}f$, such that the actual error Ef satisfies

$$Ef = |\mathcal{Q}f - \mathcal{I}f| \le \mathcal{E}f \le \mathcal{A}f,$$

where $\mathcal{A}f$ is the requested (absolute) accuracy.

An adaptive integration procedure relies on partitioning the domain to gain accuracy, especially in the vicinity of singularities. An adaptive strategy is generally based on a meta-algorithm of the type shown in Fig. 2. The subdivisions are performed in a loop that runs while the termination conditions are not yet achieved.

```
Evaluate initial region and update results
Initialize priority queue with initial region
while (evaluation limit not reached and
       estimated error too large)
    Retrieve region from priority queue
    Split region into subregions
    Evaluate new subregions and update results
    Insert new subregions into priority queue
```

Fig. 2. Adaptive Integration Meta-Algorithm

Iterated integration allows multivariate integration routines to apply one- or low-dimensional strategies in consecutive coordinate directions. For the computations in this paper, we made ample use of the QUADPACK routine DQAGSE [19], which adds an extrapolation cycle around the adaptive partitioning strategy [5,10,19].

4 Results

In the numerical computation, we take the value of $m = 1$, so that the value of s hereafter is in the unit of m^2.

4.1 Results for s-Independent Part

Table 2. s-independent part (constant value) obtained by Mathematica INTEGRATE function

Integral	C_{-1} real of I_0	C_0 real of I_1
$\mathcal{I}_{12534}$	$\frac{1}{4}\log\left(\frac{4}{3}\right) = 0.07192051811294521$	Eq. (18) $= -0.013612949401830665$

We give results of the s-independent part obtained by the Mathematica INTEGRATE function and of the s-dependent part by DQAGSE. For example, results of the s-independent part for $\mathcal{I}_{12534}$ are presented in Table 2. The s value corresponding to the threshold can be derived for each region. It was also obtained as $s = 4$ for $\mathcal{I}_{51234}$ in [7]. An imaginary part emerges for s above the threshold.

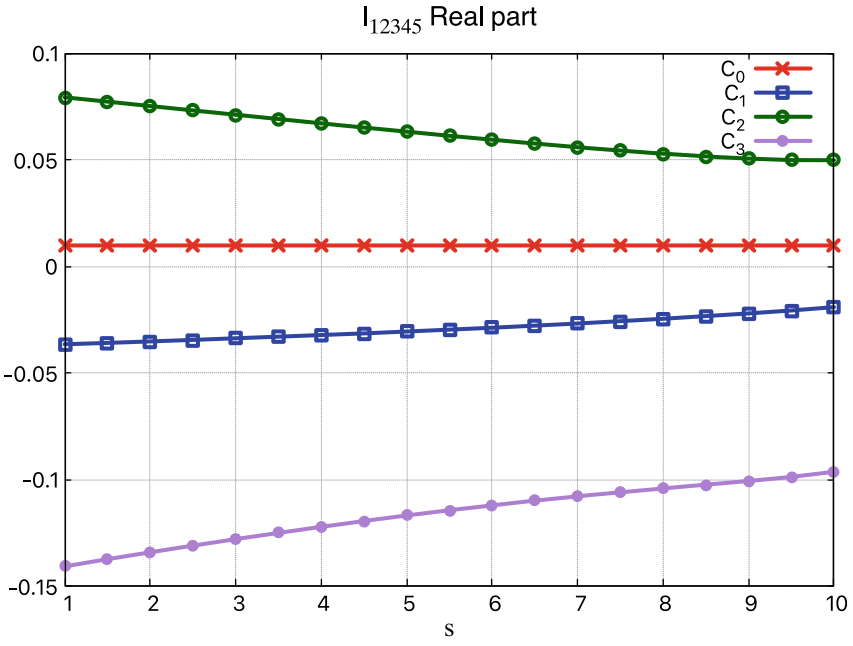

Fig. 3. Expansion coefficients for (real part) integral $\mathcal{I}_{12345}$ for $1 \leq s \leq 10$.

Table 3. C_1 values real part for $\mathcal{I}_{12345}$

s	C_1 real	C_1 err. est.	avg. time per extrapolation [sec]
1.0	−0.366254912683067133E-01	0.694E-17	0.435671
2.0	−0.352734663409193724E-01	0.694E-17	0.339906
3.0	−0.338343803945274912E-01	0.338E-19	0.349586
4.0	−0.322942491257907777E-01	0.694E-17	0.358567
5.0	−0.306349922082456046E-01	0.104E-16	0.367252
6.0	−0.288324846083721949E-01	0.694E-17	0.381545
7.0	−0.268531677116918728E-01	0.269E-19	0.433463
8.0	−0.246475664169333170E-01	0.243E-16	0.428521
9.0	−0.221359473140998880E-01	0.347E-17	0.435893
10.0	−0.191666104338030566E-01	0.153E-15	1.9738
11.0	−0.153079145751799286E-01	0.306E-09	2339.34
12.0	−0.101543652050236598E-01	0.328E-08	21444.5

Table 4. C_1 values imaginary part for $\mathcal{I}_{12345}$.

s	C_1 imag.	C_1 err. est.	avg. time per extrapolation [sec]
1.0	−0.539335522750480990E-18	0.166E-18	0.351519
2.0	−0.195362252749212056E-18	0.132E-18	0.423981
3.0	−0.246070315045975660E-18	0.424E-18	0.34778
4.0	0.104498913122451924E-17	0.633E-18	0.315143
5.0	0.192999922779541645E-17	0.694E-17	0.316811
6.0	0.348030100973042225E-18	0.351E-19	0.306804
7.0	0.114283270307553195E-17	0.830E-18	0.292358
8.0	−0.173579618677075613E-17	0.125E-18	0.293527
9.0	−0.941990468210273017E-18	0.145E-18	0.367719
10.0	0.931979443642864929E-17	0.665E-17	3.25767
11.0	0.102394384403092849E-03	0.710E-10	9435.61
12.0	0.142349044122052379E-02	0.134E-10	58581.9

A general expression (valid for C_0 real of I_1) is

$$\frac{1}{4}[-36\log 2 - 2\log^2 2 + 8\log 3 + \log 2\log 3 + 10\log 5 \\ -2\mathrm{Li}_2\left(\frac{1}{6}\right) - 2\mathrm{Li}_2\left(\frac{1}{4}\right) + 3\mathrm{Li}_2\left(\frac{1}{3}\right)] \tag{18}$$

where $\mathrm{Li}_2(z)$ is the Spence function defined as $\mathrm{Li}_2(z) = -\int_0^z \frac{\ln(1-x)}{x}\,dx$.

4.2 Results for s-Dependent Part

For $\mathcal{I}_{12345}$, Fig. 3 shows results for the expansion coefficients C_0, C_1, C_2, C_3 of the error expansion using a composite lattice rule $Q_m = Q_2$ where two scaled copies of the rule are applied in each coordinate direction. The integral is real in the range $1 \leq s \leq 10$ up to the threshold of the squared momentum, and the coefficients show a smooth behavior.

Tables 3 and 4 give numerical values for the C_1 coefficient of $\mathcal{I}_{12345}$ for $s = 1.0, \ldots, 12.0$. The threshold can be seen at $s = 10$, where the imaginary part emerges. These are computed by the DQAGSE. The computation of Feynman integrals generally becomes more time-consuming for s above the threshold. Even after performing SD of a Feynman integral, this property remains valid in each resulting regional integral. Our results, as shown in the tables, agree with this observation. Note, however, that the thresholds of the integrals obtained after sector decomposition may differ from those of the original Feynman integral. In case of $\mathcal{I}_{12345}$ the threshold is 10 and the computation time above the threshold is significantly long.

Figure 4 and Fig. 5 plot the real and imaginary parts, respectively, for the coefficients C_0 and C_1 of $\mathcal{I}_{12534}$. A threshold can clearly be seen at $s = 8$, where the imaginary part emerges. The integrations were performed adaptively with DQAGSE from QUADPACK [19], iterated for the integration over the 5D unit cube in Eqs. (6-7).

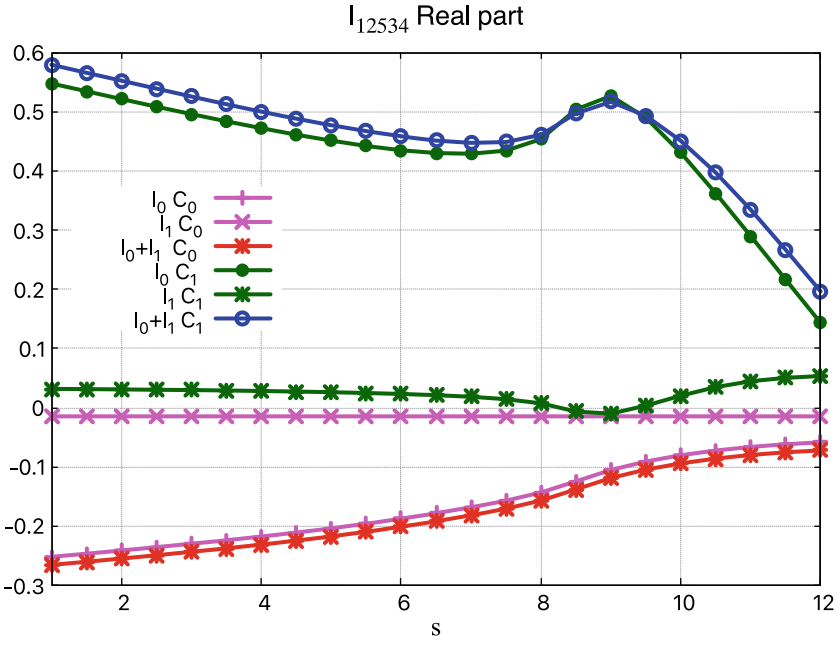

Fig. 4. Real part of expansion coefficients for integral $\mathcal{I}_{12534}$ as a function of s

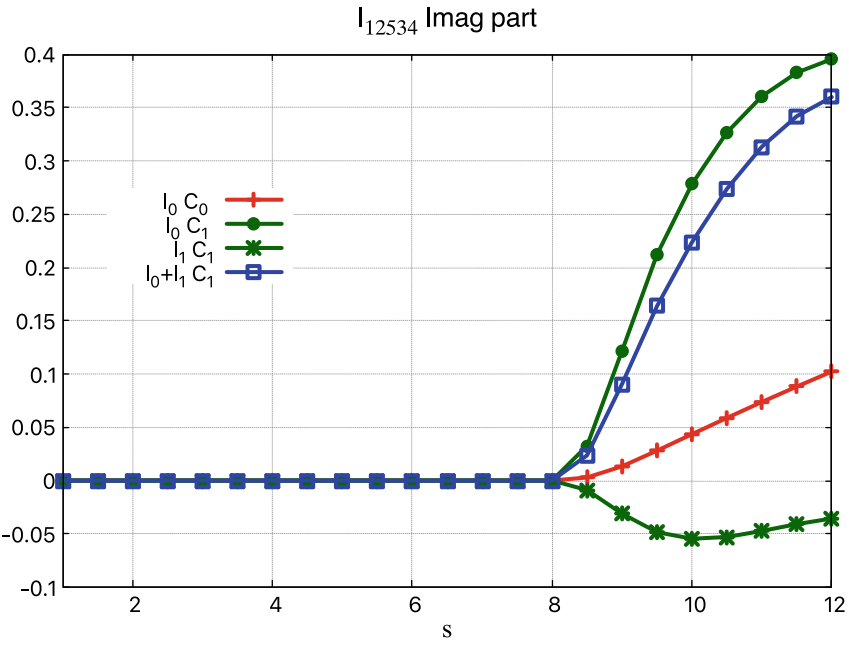

Fig. 5. Imaginary part of expansion coefficients for integral $\mathcal{I}_{12534}$ as a function of s

5 Conclusions

Higher-order corrections can contribute to accurate theoretical predictions of the cross section of particle interactions, which are fundamental to match increased accuracy in high energy physics experiments. The dimensionality and degree of difficulty increases with the number of loops and lines in the diagram. Since it is generally not possible to treat multi-loop instances with arbitrary masses and momenta, numerical approaches – in particular for higher-dimensional numerical integration in the presence of singularities, are needed to offer solutions. Lattice rules with suitable transformations provide an important tool for boundary singularities. In future work, we plan on further parallelizations of adaptive integration. We are also planning on the full computation of the 15 contributing integrals and the overall Feynman integral associated with the baseball diagram.

Acknowledgments. We acknowledge the support by JSPS KAKENHI Grant Number JP20K11858, JP20K03941 and JP21K03541. We also thank the referees for their valuable comments and suggestions.

References

1. Almulihi, A., de Doncker, E.: Accelerating high-dimensional integration using lattice rules on GPUs. In: Proc. 2017 Int. Conf. on Computational Science and Computational Intelligence (CSCI'17). CPS IEEE (2017)

2. Borowka, S., Heinrich, G., Jahn, S., Jones, S. P., Kerner, M., Schlenk, J.: A GPU compatible quasi-monte carlo integrator interfaced to pySecDec. Comput. Phys. Commun. **240**, 120–137 (2019). arXiv:1811.11720
3. Cvitanović, P., Kinoshita, T.: Feynman-Dyson rules in parametric space. Phys. Rev. D **10**, 3978 (1974)
4. de Doncker, E., Almulihi, A., Yuasa, F.: High speed evaluation of loop integrals using lattice rules. J. Phy. Conf. Ser. (JPCS) IOP Series **1085**(052005) (2018). http://iopscience.iop.org/article/10.1088/1742-6596/1085/5/052005
5. de Doncker, E., et al.: Quadpack computation of Feynman loop integrals. J. Comput. Sci. (JoCS) **3**(3), 102–112 (2011). https://doi.org/10.1016/j.jocs.2011.06.003
6. de Doncker, E., Ishikawa, T., Kato, K., Yuasa, F.: Analytic and numerical approaches for depictive 3-loop integrals using sector decomposition. Prog. Theor. Exp. Phys. **083B08** (2024). https://doi.org/10.1093/ptep/ptae122
7. de Doncker, E., Yuasa, F., , Ishikawa, T., Kato, K.: 3-loop Feynman integral extrapolations for the baseball diagram. In: (2024) the 22nd International Workshop on Advanced Computing and Analysis Techniques in Physics Research (ACAT 2024). Accepted. arXiv:2408.6551 [hep-ph]
8. de Doncker, E., Yuasa, F.: Self-energy Feynman diagrams with four loops and 11 internal lines. Springer Lecture Notes Comput. Sci. (LNCS) **12953**, 160–175 (2021)
9. de Doncker, E., Yuasa, F., Kapenga, J., Olagbemi, O.: Scalable software for multivariate integration on hybrid platforms. In: Conference on Computational Physics (CCP 2014), vol. 640. The Journal of Physics: Conf. Series (JPCS) (2015). https://doi.org/10.1088/1742-6596/640/1/012062
10. de Doncker, E., Yuasa, F., Kato, K., Ishikawa, T., Kapenga, J., Olagbemi, O.: Regularization with numerical extrapolation for finite and UV-divergent multi-loop integrals. Comput. Phys. Commun. **224**, 164–185 (2018). arXiv:1702.04904
11. de Doncker, E., Yuasa, F., Olagbemi, O., Ishikawa, T.: Large scale automatic computations for Feynman diagrams with up to five loops. Springer Lecture Notes Comput. Sci. (LNCS) **12253**, 145–162 (2020)
12. Hahn, T., Pérez-Victoria, M.: Automated one-loop calculations in four and D dimensions. Comput. Phys. Commun. **118**(2–3), 153–165 (1999). hep-ph/9807565
13. 't Hooft, G., Veltman, M.: Scalar one-loop integrals. Nucl. Phys. B **153**, 365–401 (1979)
14. Korobov, N.M.: The approximate computation of multiple integrals. Dokl. Akad. Nauk SSSR **124**, 1207–1210 (1959). (Russian)
15. Korobov, N.M.: Properties and calculation of optimal coefficients. Doklady Akademii Nauk SSSR 132, 1009–1012,: Russ. Eng. trans. Soviet Math. Doklady **1**, 696–700 (1960)
16. Nakanishi, N.: General integral formula of perturbation term in the quantized field theory. Prog. Theor. Phys. **17**, 401–418 (1957)
17. Nuyens, D., Cools, R.: Fast algorithms for component-by-component construction of rank-1 lattice rules in shift-invariant reproducing kernel Hilbert spaces. Math. Comp. **75**, 903–920 (2006)
18. Nuyens, D., Cools, R.: Fast component-by-component construction of rank-1 lattice rules with a non-prime number of points. J. Complex. **22**, 4–28 (2006)
19. Piessens, R., de Doncker, E., Überhuber, C.W., Kahaner, D.K.: QUADPACK, A Subroutine Package for Automatic Integration, Springer Series in Computational Mathematics, vol. 1. Springer-Verlag (1983)
20. Sidi, A.: A new variable transformation for numerical integration. Int. Ser. Numer. Math. **112**, 359–373 (1993)
21. Sidi, A.: Extension of a class of periodizing transformations for numerical integration. Math. Comp. **75**(253), 327–343 (2005)
22. Sloan, I., Joe, S.: Lattice Methods for Multiple Integration. Oxford University Press (1994)